ISSN 1063-7745, Crystallography Reports, 2018, Vol. 63, No. 3, pp. 344–348. © Pleiades Publishing, Inc., 2018.
Original Russian Text © A.P. Dudka, 2018, published in Kristallografiya, 2018, Vol. 63, No. 3, pp. 394–399.

STRUCTURE OF INORGANIC COMPOUNDS

First Russian Crystallographic Congress

X-Ray Structure Investigation of $Sr_3NbGa_3Si_2O_{14}$ Langasite Family Crystal

A. P. Dudka

Shubnikov Institute of Crystallography, Federal Scientific Research Centre "Crystallography and Photonics," Russian Academy of Sciences, Moscow, 119333 Russia

e-mail: dudka@ns.crys.ras.ru

Received April 24, 2017

Abstract—An accurate structure analysis of $Sr_3NbGa_3Si_2O_{14}$ single crystals, belonging to the langasite family, has been performed. Two datasets are obtained on an Xcalibur S diffractometer equipped with a CCD detector. The structure is been refined using an averaged dataset: sp. gr. $P321$, $Z = 1$, 295 K, $\sin\theta/\lambda \le 1.35$ Å^{-1}, $a = 8.2797(3)$ Å, $c = 5.0774(5)$ Å; the agreement factors between the model and experiment are found to be $R/wR = 0.76/0.64\%$ and $\Delta\rho_{min}/\Delta\rho_{max} = -0.21/0.17$ e/Å^3 for 3820 independent reflections. The $Sr_3NbGa_3Si_2O_{14}$ and $Sr_3NbFe_3Si_2O_{14}$ structures are compared, and the role of magnetic ions in the predicted $P321 \rightarrow P3$ phase transition is analyzed.

DOI: 10.1134/S1063774518030070

INTRODUCTION

$Sr_3NbGa_3Si_2O_{14}$ (SNGS) crystals belong to the langasite family; langasite is an abbreviated name of the $La_3Ga_5SiO_{14}$ crystal (structure type $Ca_3Ga_2Ge_4O_{14}$, sp. gr. $P321$, $Z = 1$ [1, 2]). Langasite crystals are of great interest due to their unique piezoelectric and nonlinear optical properties [3, 4]. Four cations (Sr, Nb, Ga, and Si) determine the SNGS structure: the Sr atom on symmetry axis 2 occupies the 3*e* Wyckoff position, the Nb atom at the intersection of symmetry axes 3 and 2 is located at the 1*a* site, the Ga atom on symmetry axis 2 is at the 3*f* site, and the Si atom on symmetry axis 3 is at the 2*d* site. Three more sites, one on symmetry axis 3 (2*d*) and two general sites (6*g*), are occupied by oxygen atoms.

In the recent years, the attention of researchers has been focused on the compounds of this family that contain magnetic cations [5, 6]: langasites, in which iron ions occupy 3*f* sites, exhibit antiferromagnetic ordering with a Neel temperature T_N of about 30 K ($T_N = 26$ K for $Sr_3NbFe_3Si_2O_{14}$ (SNFS) [6]), due to which these crystals acquire multiferroic properties [7, 8]. The occurrence of magnetic ordering in iron-containing langasites is related to the structural transition $P321 \rightarrow P3$ (loss of twofold symmetry axes), which is believed to occur below the Neel point [6]. However, since the structural studies on polycrystals [6] were insufficiently accurate, this transition has not been revealed. An analysis of the versions of phase transitions in langasite family crystals [9] indicates that, in the general case, one can hardly reach such a low temperature to implement the aforementioned transition in these crystals.

However, if a crystal contains magnetic ions, additional interatomic interaction arises in it, which may induce this transition. Therefore, a comparative analysis of structures with and without magnetic ions (e.g., SNFS and SNGS) would be useful. The prerequisites are as follows. It has been established that the magnetic moments of iron ions at 3*f* sites form a magnetic helix [6] as a result of indirect exchange interaction [8]. This helix was found to be based on a structural helix, which forms the electron density of cations at the 3*f* site and anions O3(6*g*) [10, 11]. Therefore, an analysis of the differences in the structural helices in SNGS and SNFS may yield useful information about the interatomic interaction and gain insight into the nature of the phase transition.

The purpose of this study was to develop an accurate model of the atomic structure of SNGS crystal and analyze the differences in the SNGS and SNFS structures [12]. The following question is of interest: is the interatomic interaction in the vicinity of structural helix in the SNFS crystal, which exhibits magnetic ordering, indeed stronger than in SNGS?

Table 1. Crystallographic characteristics, details of the X-ray experiment, and parameters of the $Sr_3NbGa_3Si_2O_{14}$ crystal structure refinement

Experiment	I	II
T, K	295	295
Sample shape and sizes measured in optical microscope, mm	Ellipsoid, 0.19–0.21	
Calculated sample sizes, mm	0.190(1) 0.200(1) 0.208(1)	0.190(1) 0.210(1) 0.214(1)
System, sp. gr., Z	Trigonal, $P321$, 1	
a, c, Å	8.27934(3), 5.07693(2)	8.27999(4), 5.07787(2)
c/a	0.61320	0.61327
V, Å^3	301.386(4)	301.489(5)
μ, mm^{-1}	20.97	
Diffractometer	Xcalibur S	
Radiation; λ, Å	MoK_α; 0.71073	
θ_{max}, deg	74.1	74.2
Ranges of indices h, k, l	$-21 \le h \le 22$, $-20 \le k \le 19$, $-13 \le l \le 13$	$-20 \le h \le 21$, $-19 \le k \le 19$, $-13 \le l \le 11$
Number of reflections: measured/unique with $F^2 \ge 2\sigma(F^2)$	47131/3883	37182/3592
Number of rejected unique reflections, $F^2 < 2\sigma(F^2)$	301	484
Redundancy	11.26	9.12
$\langle\sigma(F^2)/F^2\rangle$	0.041	0.055
$R1_{av}(F^2)/wR2_{av}(F^2)$, %	1.96/2.17	2.55/3.88
Number of refined parameters	74	74
$R1(\|F\|)/wR2(\|F\|)$, %	0.759/0.674	0.974/0.846
S	1.013	1.033
$\Delta\rho_{min}/\Delta\rho_{max}$, e/Å^3	−0.18/0.20	−0.32/0.20
Refinement based on cross-data set		
Number of reflections/parameters	3820/72	
$R12_{av}(\|F\|)/wR12_{av}(\|F\|)$, %	1.094/0.970	
$R1(\|F\|)/wR2(\|F\|)$, %	0.756/0.644	
S	0.903	
$\Delta\rho_{min}/\Delta\rho_{max}$, e/Å^3	−0.21/0.17	

Programs in use: CrysAlisPro [13] and ASTRA [15]. $\langle a\rangle$ = 8.2797(3) Å, $\langle c\rangle$ = 5.0774(5) Å; $R12_{av}$ is the R factor for averaging identical reflections from two data sets merged into a cross-data set; $R1(|F|) = \sum||F_{obs}| - |F_{calc}||/\sum|F_{obs}|$; $wR2(|F|) = \sqrt{\left\{\sum w(|F_{obs}| - |F_{cals}|)^2/\sum w(F_{obs})^2\right\}}$.

EXPERIMENTAL

A fine-grained SNGS aggregate was pulled from a melt of stoichiometric composition by the Czochralski method. The sample for diffraction analysis had a shape of a nonideal sphere. Two sets of diffraction reflection intensities were collected on a Xcalibur S3 diffractometer (Rigaku Oxford Diffraction) equipped with a CCD detector. The details of data collection and SNGS structure refinement are listed in Table 1. The crystallographic data were deposited with the Inorganic Crystal Structure Database (ICSD) (CSD no. 433693).

The reciprocal space was covered by more than 99.7% with a resolution of $(\sin\theta/\lambda)_{max}$ = 1.35 Å^{-1} in the experiments. The integrated intensities were obtained according to [13]. Data processing and structure model refinement were performed using the ASTRA program [14, 15]: corrections were introduced for the thermal diffuse scattering [16] with elastic constants taken from [17], the X-ray absorption for ellip-

Table 2. Atomic coordinates, site occupancies Q, equivalent thermal parameters U_{eq}, and ellipsoidality ε of atomic displacements in the $Sr_3NbGa_3Si_2O_{14}$ crystal

Atom	Site	*x/a*	*y/b*	*z/c*	*Q*	U_{eq}, Å^2	ε
Sr	3*e*	0.42903(1)	0	0	1.0	0.01061(2)	0.004053
Nb	1*a*	0	0	0	1.0	0.0086(1)	0.005152
Ga	3*f*	0.74718(1)	0	1/2	1.0	0.00908(8)	0.006542
Si	2*d*	1/3	2/3	0.53496(3)	1.0	0.0083(3)	0.001438
O1	2*d*	1/3	2/3	0.22088(8)	1.0	0.0130(3)	0.015638
O2	6*g*	0.47383(7)	0.30711(9)	0.3321(1)	1.0	0.01324(7)	0.026394
O3	6*g*	0.22114(4)	0.09320(4)	0.76883(5)	1.0	0.01264(6)	0.026250

soidal samples [18, 19], the diffractometer calibration [20, 21], the extinction effect [22, 23], and the half-wavelength contribution [24]. Friedel pairs were not averaged. The structure model (Table 2) contains the atomic displacement ellipsoidality ε [11]. It was refined according to the cross-set obtained by averaging of measurements from two datasets to compensate for systematic errors using the intermeasurement minimization method [25].

RESULTS AND DISCUSSION

To justify the comparison of the structure models of SNGS and SNFS crystals [12], data were processed and structure models were refined as similarly as possible. A refinement of the SNGS structure revealed that this crystal has a right-handed [26] single-domain enantiomorphic configuration (as well as SNFS).

The standard model of spherical atoms in the harmonic approximation of atomic displacements in langasite structure includes 39 parameters. However, this model reveals significant residual peaks near atoms in difference electron-density maps. The observed disordering of atomic sites in the SNGS structure was described using the model of anharmonic atomic displacements [27, 28]. In correspondence with [29], the constructed SNGS model is denoted as 4242232. Its difference from the 4232234 model for SNFS at 295 K is small but noticeable. The disordering of Sr(3*e*) and (Ga or Fe)(3*f*) cation sites and O2(6*g*) anion site is similar in these crystals, but SNFS exhibits additional features for the O3(6*g*) site (the fourth rank tensor of atomic displacements), through which indirect exchange interaction occurs along the Fe(3*f*)–O3(6*g*)–O3(6*g*)–Fe(3*f*) helix. The spread of electron density along the line of this helix is very strong in SNFS [12] and moderate in SNGS (Fig. 1).

Despite the small difference in the ionic radii [$r(Ga^{3+}_{IV}/Fe^{3+}_{IV})$ = 0.47/0.49 Å], the effect of replacement of Ga with Fe in the 3*f* tetrahedron is rather significant and somewhat paradoxical. These changes become most pronounced when comparing the four main polyhedra of the structure [12]. Rigid silicon 2*d* tetrahedra do not affect much the characteristics of structural helix: the Ga → Fe replacement shifts them upwards along the *c* axis as a single whole (Fig. 2a).

It was assumed a priori that the volume of the Sr(3*e*) polyhedron in SNFS is smaller than in SNGS, because the Ga → Fe replacement leads to an expected increase in the volume of 3*f* tetrahedron from 3.109(1) Å^3 [Ga(3*f*)] to 3.221(3) Å^3 [Fe(3*f*)], and it should compress the Sr(3*e*) polyhedron in SNFS from above. However, Fig. 2b shows that the Sr(3*e*) polyhedron is, vice versa, larger in SNFS, and its volume increases from 30.847(5) Å^3 (in SNGS) to 31.08(1) Å^3 (in SNFS).

One might suggest that this situation is caused by a competing effect: magnetic exchange interaction in the vicinity of helix. Indeed, the Fe(3*f*) and O3(6*g*) atoms in SNFS are located closer to the *c* axis of the unit cell (to the helix axis) than Ga(3*f*) and O3(6*g*) in SNGS (Fig. 2c). The volume of the 1*a* octahedron, located on the helix axis, is much lower in SNFS than in SNGS (10.223(1) → (10.058(6) Å^3), and the degree of twist of the O3(6*g*) atoms located on the helix line

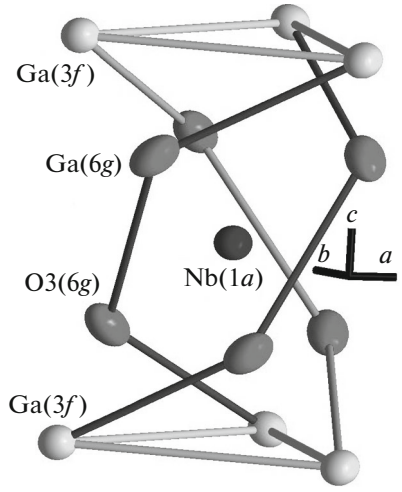

Fig. 1. Fragment of electron density helix Ga(3*f*)–O3(6*g*)–O3(6*g*)–Ga(3*f*), imitating the threefold screw symmetry axis in SNGS crystal.

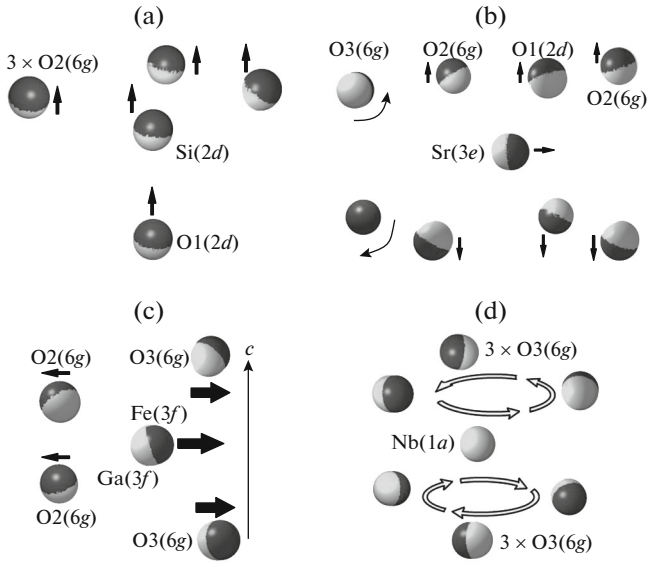

Fig. 2. Comparison of the atomic positions in SNGS and SNFS polyhedra (arrows indicate the results of Ga → Fe replacement): (a) silicon 2*d* tetrahedra have close volumes; (b) the Sr(3*e*) polyhedron in SNGS has a smaller volume than in SNFS; (c) the Fe(3*f*) and O3(6*g*) atoms in SNFS are closer to the cell axis *c* (i.e., to the helix axis) than the Ga(3*f*) and O3(6*g*) atoms in SNGS; and (d) the SNFS polyhedron exhibits an additional (in comparison with SNGS) twist of the O3(6*g*) atoms located on the helix line, while the volume of the niobium 1*a* octahedron in SNFS is much smaller than in SNGS. The atoms in SNGS and iron-containing SNFS are given in lighter and darker tones, respectively.

in SNFS increases (Fig. 2d). In other words, one might suggest that the expansion of the Sr(3*e*) polyhedron in the SNFS structure becomes possible due to the "magnetic" compression of the neighboring 1*a* octahedron and, correspondingly, the structural helix, despite the larger sizes of the Fe(3*f*) tetrahedron.

Thus, the results of this study evidenced that the diameter of the Fe(3*f*)–O3(6*g*)–O3(6*g*)–Fe(3*f*) structural helix in the iron-containing crystal SNFS is smaller than the diameter of the Ga(3*f*)–O3(6*g*)–O3(6*g*)–Ga(3*f*) helix in SNGS, although the size of Fe ion somewhat exceeds that of Ga ion. The iron and oxygen ions in the vicinity of helix in SNFS are located closer; i.e., Fe ions in SNFS are more strongly bonded than Ga ions in SNGS. It is reasonable to suggest that this proximity of Fe ions is caused by their magnetic interaction, because other structural differences appear insignificant. When an SNFS crystal is cooled, this interaction is enhanced, as evidenced by further approaching of iron ions [12]. Finally, at the Neel temperature, the quantitative changes become qualitative, and SNFS exhibits magnetic ordering [6]. The results obtained give grounds to expect that the related *P*321 → *P*3 phase transition can be observed in a carefully prepared low-temperature helium experiment.

CONCLUSIONS

Accurate X-ray structure analysis of $Sr_3NbGa_3Si_2O_{14}$ crystal was performed using an averaged dataset: sp. gr. *P*321, $Z = 1$, $\sin\theta/\lambda \le 1.35$ Å^{-1}, 295 K; $a = 8.2797(3)$ Å, $c = 5.0774(5)$ Å; $R/wR = 0.76/0.64\%$; and $\Delta\rho_{min}/\Delta\rho_{max} = -0.21/0.17$ e/Å^3 for 3820 unique reflections and 72 refined parameters. The $Sr_3NbGa_3Si_2O_{14}$ and $Sr_3NbFe_3Si_2O_{14}$ structures are compared, and the role of magnetic ions in the predicted *P*321 → *P*3 phase transition is analyzed. It is shown that the atoms forming the structural helix Fe(3*f*)–O3(6*g*)–O3(6*g*)–Fe(3*f*) in SNFS are located more compactly than the atoms of the similar helix in SNGS. This compactness, which may be due to the indirect exchange interaction in SNFS, is likely a precursor of the *P*321 → *P*3 phase transition.

ACKNOWLEDGMENTS

I am grateful to B.V. Mill' for supplying SNGS crystals.

This work was supported by the Federal Agency of Scientific Organizations (Agreement No 007-ГЗ/Ч3363/26) and was performed using equipment of the Shared Research Center of the Shubnikov Institute of Crystallography of Federal Scientific Research Centre "Crystallography and Photonics" of the Russian Academy of Sciences.

REFERENCES

1. E. L. Belokoneva and N. V. Belov, Dokl. Akad. Nauk SSSR, **260** (6), 1363 (1981).
2. E. L. Belokoneva, S. Yu. Stefanovich, Yu. V. Pisarevskii, et al., Russ. J. Inorg. Chem. **45** (11), 1642 (2000).
3. A. A. Kaminsky, B. V. Mill', S. E. Sarkisov, et al., *Physics and Spectroscopy of Laser Crystals* (Nauka, Moscow, 1986) [in Russian], p. 197.
4. B. V. Mill and Yu. V. Pisarevsky, *Proc. IEEE/EIA Int. Frequency Control Symp., Kansas City, Missouru, USA, 2000,* p. 133.
5. V. Yu. Ivanov, A. A. Mukhin, A. S. Prokorov, and B. V. Mill, Solid State Phenom. **152–153**, 299 (2009).
6. K. Marty, P. Bordet, V. Simonet, et al., Phys. Rev. B **81**, 054416 (2010).
7. I. S. Lyubutin, P. G. Naumov, B. V. Mill', et al., Phys. Rev. B **84**, 214425 (2011).
8. S. A. Pikin and I. S. Lyubutin, Phys. Rev. B **86**, 4414 (2012).
9. B. V. Mill', B. A. Maksimov, Yu. V. Pisarevskii, et al., Crystallogr. Rep. **49** (1), 60 (2004).
10. A. P. Dudka and B. V. Mill', Crystallogr. Rep. **58** (4), 594 (2013).
11. A. P. Dudka and B. V. Mill', Crystallogr. Rep. **59** (5), 689 (2014).
12. A. P. Dudka and A. M. Balbashov, *18th Int. Conf. on Crystal Growth and Epitaxy (ICCGE-18), Nagoya, Japan, August 7–12, 2016,* p. 36.

13. *Oxford Diffraction. Xcalibur CCD System, CrysAlisPro Software System, Version 1.171.32* (Oxford Diffraction Ltd., 2007).
14. A. P. Dudka, Crystallogr. Rep. **47** (1), 152 (2002).
15. A. Dudka, J. Appl. Crystallogr. **40**, 602 (2007).
16. A. P. Dudka, M. Kh. Rabadanov, and A. A. Loshmanov, Kristallografiya **34** (4), 818 (1989).
17. A. V. Sotnikov, R. Kunze, H. Schmidt, et al., Phys. Solid State **51** (2), 275 (2009).
18. A. P. Dudka, Crystallogr. Rep. **50** (6), 1068 (2005).
19. A. P. Dudka, Crystallogr. Rep. **51** (1), 157 (2006).
20. A. Dudka, J. Appl. Crystallogr. **43** (6), 1440 (2010).
21. A. P. Dudka, Crystallogr. Rep. **60** (4), 601 (2015).
22. P. J. Becker and P. Coppens, Acta Crystallogr. A **30**, 129 (1974).
23. Page. Y. Le and E. J. Gabe, J. Appl. Crystallogr. **11**, 254 (1978).
24. A. Dudka, J. Appl. Crystallogr. **43**, 102 (2010).
25. A. P. Dudka, Crystallogr. Rep. **47** (1), 152 (2002).
26. V. N. Molchanov, B. A. Maksimov, D. F. Kondakov, et al., JETP Lett. **74** (4), 222 (2001).
27. P. I. Kuznetsov, R. L. Stratonovich, and V. I. Tikhonov, Teor. Veroyatn. Ee Primen. **5** (1), 84 (1960).
28. C. K. Johnson, Acta Crystallogr. A **25**, 187 (1969).
29. A. P. Dudka and B. V. Mill', Crystallogr. Rep. **56** (3), 443 (2011).

Translated by Yu. Sin'kov